VERIZONA PUBLISHER
Publishing Your Ideas

www.verizonaonlinepublishing.com
Vol: 1, Issue: 3

Journal of Nanoscience with Advanced Technology

One-pot Synthesis of Size Controllable Amine-Functionalized Core-Shell Magnetic Nanoparticles for Use in Microfluidic Flow Separators

Xia Chen[1], Michael G. Organ[1] and William J. Pietro[1,*]

Department of Chemistry, York University, 4700 Keele St. Toronto, ON M3J 1P3, Canada

***Corresponding author:** William J. Pietro, Department of Chemistry, York University, 4700 Keele St. Toronto, ON M3J 1P3, Canada; Tel: +1(416)-736-2100 ext: 77700 (L 77720); E mail: pietro@yorku.ca

Article Type: Research, **Submission Date**: 10 December 2015, **Accepted Date:** 07 January 2016, **Published Date:** 27 January 2016.

Citation: Xia Chen, Michael G. Organ and William J. Pietro (2016) One-pot Synthesis of Size Controllable Amine-Functionalized Core-Shell Magnetic Nanoparticles for Use in Microfluidic Flow Separators. J Nanosci Adv Tech 1(3): 25-31. doi: https://doi.org/10.24218/jnat.2016.14.

Abstract

Silica coating of magnetic nanoparticles has been widely used as a surface modification strategy to endow various surface functionalization and fast magnetic respond for application in molecular separation and purification. A simple one-pot synthesis of amine functionalized core-shell magnetic nanoparticles with a tunable shell thickness has been prepared in a reverse microemulsion system. The morphologies and sizes of resulting nanoparticles were confirmed by PXRD spectroscopy and TEM imaging. Nanoparticles prepared by this method are single-core dominated and highly monodisperse, and show great potential for use in a closed-cycle microfluidic magnetic purification system. To demonstrate this idea, fluorescein was used as a model carboxylate molecule to demonstrate the potential separation ability of Fe_3O_4@SiO_2-NH_2 nanoparticles towards cationic targets via UV-VIS spectroscopy. The results show that fluorescein molecules can be quickly and quantitatively associated with the magnetic nanoparticles via electrostatic binding, resulting in an average of 2.73 x 10^3 adsorbed target molecules per nanoparticle. In addition, covalent binding of target molecules to the nanoparticles is also demonstrated.

Keywords: One-pot, Iron oxide, Core-shell, Magnetic purification.

Introduction

Surface-functionalized monodisperse iron oxide magnetic nanoparticles promise great advancement in a wide range of applications, including drug delivery, [1] magnetic resonance imaging (MRI), [2,3] bioseparation of proteins, DNA and cells, [4-6] catalysis, [7,8] ferrofluids, [9] data storage, [10] and adsorption [11]. The advantages of using iron oxide over other magnetic materials include low cost, ease of preparation, biocompatibility (FDA approved material) and chemical stability [12-14]. In most applications, the performance of iron oxide nanoparticles (IONPs) greatly depends on their size and morphologies. Typically, IONPs present the unique physical property of superparamagnetism at sizes below 50 nm, meaning that each nanoparticle bears a large magnetic moment (as high as 90 emu g^{-1}) in the presence of a magnetic field, yet does not permanently magnetize once the field is removed [15-17]. In addition, the large surface-to-volume ratios can be exploited for facile heterogeneous reactions at surface functionalities. Popular synthetic approaches of IONPs include co-precipitation, [18] thermal decomposition, [19,20] microemultion, [21] and hydrothermal synthesis, [22] with yields, shapes, and size distributions varying between these various methods.

Although the co-precipitation approach is most straightforward and readily scalable, polydisperse IONPs with ill-defined shapes are typically obtained. Hydrophobic IONPs obtained by thermal decomposition has become one of the most attractive methods in recent years.[15,23] In this method, a precursor iron complex is mixed with a surface capping agent and decomposed in a high-boiling nonpolar solvent at temperatures above 300°C, resulting in iron oxide nanocrystals with very high scalability, narrow size distributions, tunable sizes and low crystalline defects. [15,24] Of course, subsequent application of those IONPs for aqueous microfluidic separations require the long hydrophobic alkyl surfactants on their surfaces be replaced by hydrophilic or amphiphilic ligands. Despite a few reports of ligand exchange or amphiphilic ligand encapsulation strategies, [25] a more facile methodology would be most welcome. A recent published work by Liu [26] that demonstrates a direct conversion from hydrophobic to hydrophilic IONPs using 3,4-dihydroxyhydrocinnamic acid without any complicated organic synthesis, is a good example.

In addition to imparting solubility properties, surface capping of IONPs prevents aggregation as a result of their high surface energies. [27,28] Moreover, target-specific surface modified magnetic nanoparticles can be used for separation and isolation of biological or chemical agents, including proteins, nucleic acids, cells, dyes, and metal ions. [29-33] Thus, a generalizable surface modification strategy is an important first step towards the application of IONPs in separation technology.

The formation of core-shell IONPs comprising a silica coating onto a single magnetic core seems attractive towards realizing this goal. Simple microemulsion methods have been reported for the facile encapsulation of a variety of nanoparticulate cores with silica shells [34-38]. Unfortunately, subsequent shell

functionalization typically involves complicated multi-step procedures and polymerizations, which are time-consuming and labor intensive [39]. Therefore, less complicated synthetic routes towards functionalized magnetic nanoparticles are desirable.

In this work we report a simple one-pot synthesis of amine functionalized core-shell magnetic nanoparticles with a tunable shell thickness using a reverse microemulsion method, and we demonstrate its potential applicability in microfluidic separations.

Experimental

Materials and methods

Ferric chloride hexahydrate ($FeCl_3 \bullet 6H_2O$, 98%) was purchased from Fisher, sodium oleate (TCI, 95%) was obtained from TCI America. Tetraethyl orthosilicate (TEOS, 98%), (3-aminopropyl) triethoxysilane (APTES, 99%), cyclohexane (≥99%), 1-butanol (≥99%), and IGEPAL®CO-520 ($(C_2H_4O)_n \cdot C_{15}H_{24}O$, n~5, average Mn 441), Fmoc chloride (97%), piperidine (99%), dimethylformamide (DMF, 99.8%), and sodium fluorescein (used as fluorescent tracer) were purchased from Sigma-Aldrich. Sodium acetate (NaOAc, anhydrous, ≥99%), Triton-X100 (laboratory grade) were bought from BDH chemicals; ammonium hydroxide (NH_4OH, 28%~30%) was obtained from Caledon. All solvents were dried over 4A molecular sieves and filtered prior to use.

UV-VIS spectroscopy was performed on a NanoDrop 2000c/2000 UV-Vis spectrophotometer. Fluorescence measurements were carried out using a NanoDrop 3300 spectrofluorimeter. High-speed centrifugation (maximum 10500 rpm) was performed using a Baxter Biofuge 17R centrifuge. Sonication was performed using a Branson 450 Digital Sonifier. A high temperature (320°C) reaction was carried out in either a Welmet FT3034 or Carbolite STF 16/180 tube furnace. A sintered $Nd_2Fe_{14}B$ permanent supermagnet was used for magnetically-assisted precipitation of nanoparticles.

Synthesis of monodisperse hydrophobic Fe_3O_4 nanoparticles

Monodisperse hydrophobic IONPs were obtained using a modification of the thermal decomposition method of Hyeon [20]. Iron oleate was first prepared by refluxing a mixture of $FeCl_3 \bullet 6H_2O$ (8 mmol, 2.16g) and sodium oleate (24 mmol, 7.31g) in a solvent mixture of H_2O, EtOH, C_6H_6 to C_6H_{14} (12 mL, 16 mL, 28 mL) at 70°C for 4 h. The expected $Fe(oleate)_3$ complex was extracted from the organic layer using a separatory funnel, washed with distilled water 3 times, and dried *in vacuo*. 4.24g (4.72 mmol) $Fe(oleate)_3$ was transferred into a 80 mL tube containing 1-octadecane (29.9 mL), oleic acid (2.36 mmol, 0.75 mL), and made homogeneous with a votex mixer. The tube was transferred to a tube furnace, and flushed with argon. The reaction mixture was heated to 320°C and refluxed at this temperature for 1 h under argon. The resulting black solution was cooled to room temperature and precipitated by excess ethanol. The precipitate was collected by centrifugation (10500 rpm), then redispersed in hexane and precipitated with ethanol several times to purify the resulting Fe_3O_4 nanoparticles. The purified IONPs were dried *in vacuo* (10 mtorr) and stored as a suspension in cyclohexane (25 mg/mL) under Ar.

One-pot synthesis of amine modified Fe_3O_4 core-shell nanoparticles with controllable shell thickness

A modification of the reverse microemulsion method of Ding, et al [37] was used to obtain amine functionalized core-shell IONPs, herein symbolized as $Fe_3O_4@SiO_2$-NH_2. Typically, 0.25 mL of the nonionic surfactant Igepal CO-520 (see chemical formula 1) was dissolved in 10 mL cyclohexane, and subjected to sonication for 15 min. Then 100 µL NH_4OH was added followed by 2.5 mg Fe_3O_4 (2.5 mg/mL in cyclohexane). After 30 min of continuous magnetic stirring, 50 µL TEOS was added to the mixture via an equivalently fractionated dropping method at a rate of 35 µL per 16 h. A certain molar ratio of APTES to TEOS was subsequently added after the TEOS was fully hydrolyzed. When the reaction finished, 2 mL of methanol was added to break the microemulsion. The hydrophilic product was purified by washing with EtOH and distilled water alternatively. The resulting $Fe_3O_4@SiO_2$–NH_2 MNPs were collected magnetically and dried *in vacuo*.

Determination of active amine groups on $Fe_3O_4@SiO_2$–NH_2 IONPs

20 mg $Fe_3O_4@SiO_2$–NH_2 were dispersed in 2 mL dry DMF. An excess amount of Fmoc-Cl (1.07 mmol, 277 mg) was added and the mixture was sonicated for 40 min under argon. The nanoparticles were isolated by high-speed centrifugation (10500 rpm), washed with MeOH 5 times to remove unattached Fmoc-Cl residues, and dried *in vacuo*. The attached Fmoc molecules were then cleaved by the action of piperidine (200 uL) in DMF (800 uL) under sonication for 20 min. The nanoparticles were removed by high-speed centrifugation (10500 rpm), and the supernatant was examined spectrophotometrically to determine the amount of Fmoc-Cl molecules that were covalently bound to the NH_2 groups.

Surface binding capacity of $Fe_3O_4@SiO_2$-NH_2 IONPs

20 mg $Fe_3O_4@SiO_2$-NH_2 IONPs were homogenously dispersed by sonication in 5 mL MQ water. The pH was then lowered to 5.0 by the dropwise addition of 0.1M HCl. Sodium fluorescein (0.54 mL, 0.01 M) was then added to the protonated IONPs as a model target carboxylate molecule, causing the pH of the suspension to jump to 9.3. The pH was then adjusted back to 5.0 with 0.1M HCl. After stirring the suspension for 1 h, fluorescein-bound IONPs were washed with anhydrous ethanol several times, magnetically separated from the suspension, and washed with water by repeated sonication/magnetic isolation cycles until the washings were free from fluorescence. The precipitated IONPs were dried *in vacuo*, then sonicated into 1000 uL NaOH (pH=11) to cleave all adsorbed fluorescein molecules from the IONPs. The unbound IONPs were then magnetically removed from suspension, and the concentration of fluorescein in solution was determined spectrofluorometrically.

Results and Discussion

Monodisperse $Fe_3O_4@SiO_2$ core-shell nanoparticles

Hydrophobically-capped iron oxide cores were prepared by the thermal decomposition of iron oleate [20]. Transmission electron microscopy (Figure 1a) confirms the material exists as highly monodisperse spherical nanoparticles having average

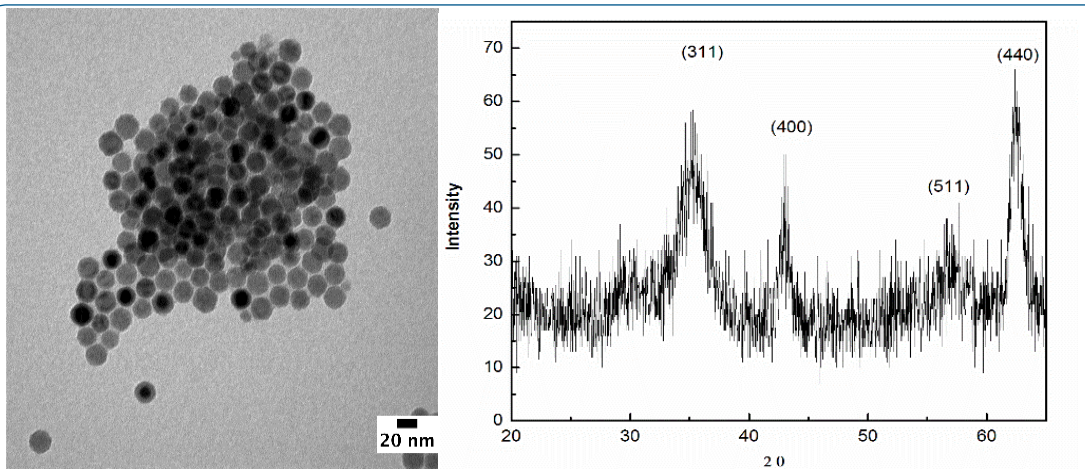

Figure 1: (a) TEM image and (b) PXRD pattern of Fe_3O_4 cores

diameter of 20 nm. Powder X-ray diffraction studies (Figure 1b) confirm that these particles are magnetite (Fe_3O_4). Application of the Scherrer equation to the broadening of the (311) reflection signal corroborate an average diameter of 20 nm.

Fe_3O_4@SiO_2 core-shell nanoparticles were obtained by silica coating the Fe_3O_4 cores through a water-in-oil (w/o) microemulsion process, [38] in which the base-catalyzed hydrolysis of tetraethyoxysilane (TEOS) occurs in the interior of reverse micelles of surfactant Igepal CO-520, 1 (average molecular weight = 441), in cyclohexane. The micelles nucleate around the Fe_3O_4 cores, promoting the growth of silica encapsulated core-shell structures. To obtain core-shell nanostructures with a single magnetic core, and without core-free SiO_2 nanoparticles, it is crucial to match the number of magnetic cores with the number of inverse micelles. It is known that the size and number of inverse micelles in a base-catalyzed silica microemulsion is governed by a complex interplay between the concentrations of base, organosilane, and surfactant. [37] At low core to micelle ratios core-free silica nanoparticles form. At high core to micelle ratios multicore structures are present. We found the optimum conditions for producing the highest yield of single-core structures with little or no core-free silica has a core:NH_4OH:CO-520 mass ratio of 2.5:0.1:250. Moreover, under these optimum conditions, we found that the thickness of the shell can be controlled by the gross amount of TEOS in the reaction mixture. For example, the addition of 50 µL and 75 µL TEOS to 2.5 mg of Fe_3O_4 cores in 10.0 mL cyclohexane gave silica shell wall thicknesses of 15 nm and 20 nm, respectively (Figure 2).

Size-tunable amine-functionalized Fe_3O_4@SiO_2-NH_2 IONPs

A series of amine terminated core-shell nanoparticles were obtained by adding a specific mole fractions of (3-aminopropyl) triethoxysilane (APTES) before breaking the reverse microemulsion system with methanol using an equivalently fractionated dropping method, as shown in Scheme 1. This resulted in predominantly single-core core-shell structures with an amine layer thickness ranging from 15 to 40 nm, controllable by the mole ratio of APTES (0 – 0.5) as shown in Figures 3 and 4. After amine modification, the surface of the nanoparticles appears to roughen, relative to the unfunctionalized core-shell systems. This may be because APTES added as a second silane source after TEOS hydrolysis, possibly nucleated small independent particles before merging onto the Fe_3O_4@SiO_2 surface.

The presence of surface amine groups was confirmed by IR spectroscopy. Figure 5 presents the IR spectra of (a) oleate capped Fe_3O_4 nanoparticles, (b) Fe_3O_4@SiO_2 core-shell nanoparticles, and (c) Fe_3O_4@SiO_2-NH_2 amine-functionalized core-shell structures (10% APTES). In spectrum (a), the absorptions at 2923 cm^{-1} and 1624 cm^{-1} are attributed to aliphatic C-H and carboxylate C=O,[40] respectively, and indicate the existence of oleic acid capping groups. The absorptions near 1099, 947, 800, and 471 cm^{-1} appear in spectra b and c, and are assigned to vibrational modes of SiO_2 [37]. The broad peak centered at 3408 cm^{-1} arises from the stretching vibration of surface Si-O-H bonds [12]. In spectrum c, two additional absorptions are observed at 3392 and 3257 cm^{-1}, and are assigned to stretching vibrations of -NH_2. [41,42] The band observed at 1506 cm^{-1} is assigned to the –NH_2 bending mode [41].

Assay of the active surface amine moieties was accomplished by a standard Fmoc quantification protocol [43] Fmoc chloride undergoes quantitative covalent binding to primary amine residues via an amide linkage. Thus, the Fe_3O_4@SiO_2-NH_2 nanoparticles were incubated with excess Fmoc chloride, then isolated and washed extensively to remove any unbound Fmoc. The Fmoc tagged nanoparticles were then suspended in clean DMF, and the amide linkage was cleaved by the action of piperidine. The concentration of free Fmoc in solution was determined spectrophotometrically, using the two predominant absorption bands of Fmoc (226 nm and 300 nm). This sequenced is summarized in Scheme 2.

Using this procedure, we determined that our Fe_3O_4@SiO_2-NH_2 has an average of $1.21 \pm 0.036 \times 10^{-7}$ mol/mg amine and 1.58×10^4 amine moieties per nanoparticle. An unfunctionalized control sample of Fe_3O_4@SiO_2 taken through Scheme 2 resulted in no detectable UV absorption at either wavelength.

Magnetic separation of anionic organic targets by Fe_3O_4@SiO_2-NH_2 nanoparticles

We demonstrate the potential of our surface-functionalized core-shell magnetic nanoparticles for use in a closed-cycle magnetic purification (CCMP) microfluidic device, by electrostatically

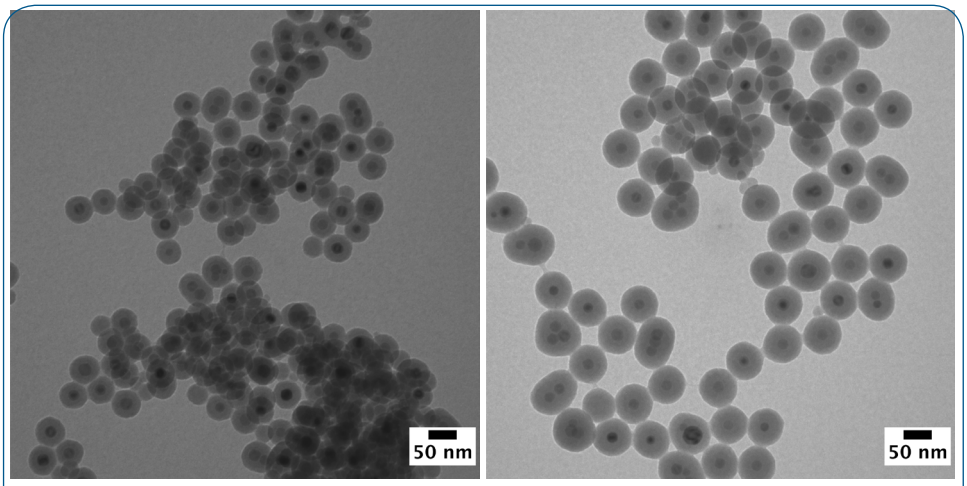

Figure 2: TEM images of Fe_3O_4@SiO_2 core-shell structures. (a) 50 µL/mg (TEOS:Fe_3O_4), (b) 75 µL/mg (TEOS:Fe_3O_4)

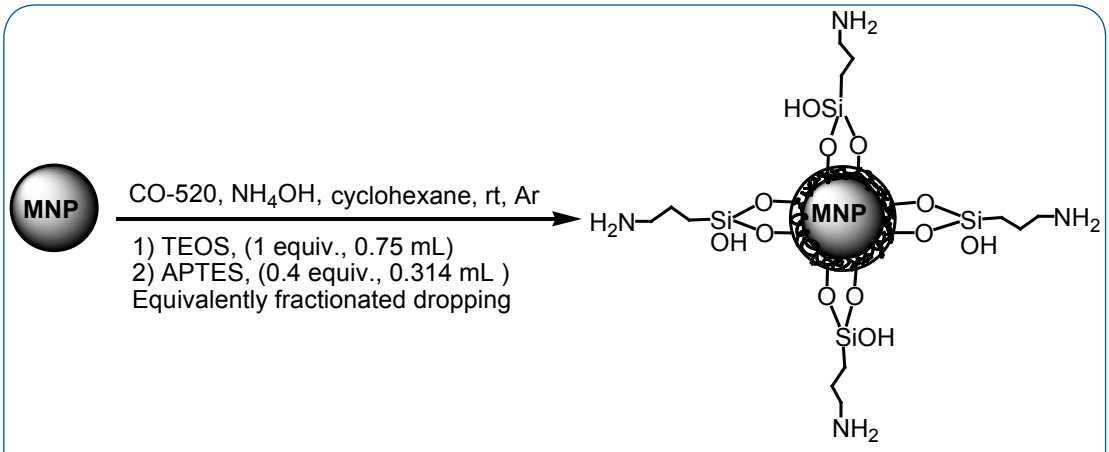

Scheme 1: One-pot synthesis of amine-functionalized Fe_3O_4@SiO_2-NH_2 magnetic nanoparticles

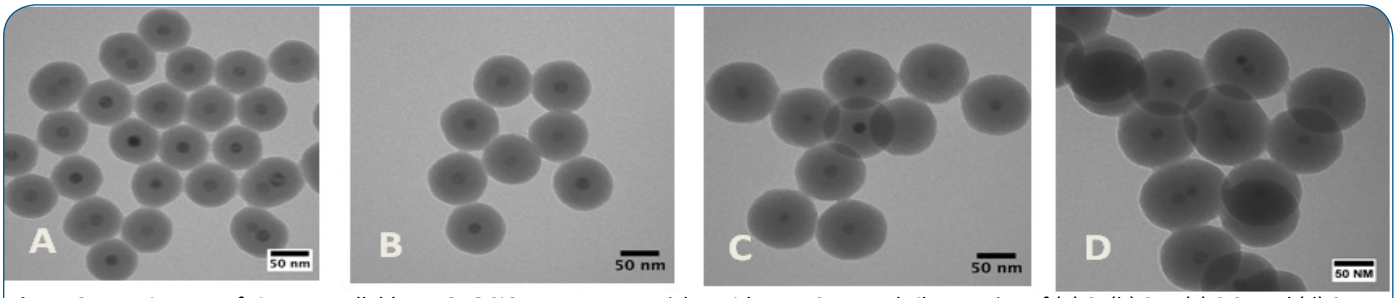

Figure 3: TEM images of size-controllable Fe_3O_4@SiO_2-NH_2 nanoparticles with APTES to total silane ratios of (a) 0, (b) 0.1, (c) 0.3, and (d) 0.5

binding fluorescein carboxylate as a model target, magnetically separating the target-nanoparticle complex from the target solution, and releasing the target into fresh solvent by pH induced desorption from the nanoparticle, as illustrated in Scheme 3. Fluorescein is a convenient model target, as its intense visible fluorescence can be readily detected by the naked eye under UV illumination, and accurately assayed fluorometrically.

The Fe_3O_4@SiO_2-NH_2 suspension is first brought to pH 5, protonating the amine surface. This suspension is then added to an aqueous solution of sodium fluorescein, in which the fluorescein exists as an anion that electrostatically adsorbs to the cationic surface of the nanoparticles. The fluorescein-bound nanoparticles are then isolated from the target solution by magnetic separation and, after several washings with ethanol to remove any unbound fluorescein, ultrasonically suspended in a clean aqueous solution. This suspension shows no visible fluorescence, indicating that the fluorescein is likely bound through its (non-fluorescent) open-ring carboxylate form. Raising the pH to 11, deprotonates the nanoparticle surface, thus releasing the fluorescein target into solution. The unbound nanoparticles were then completely removed from the supernatant by high-speed centrifugation.

At high pH, fluorescein exists in its highly fluorescent lactone-

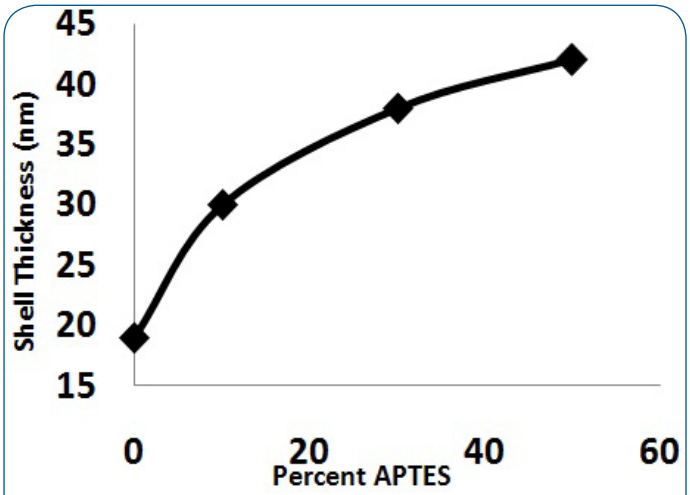

Figure 4: Average SiO_2 shell thickness dependence on APTES concentration

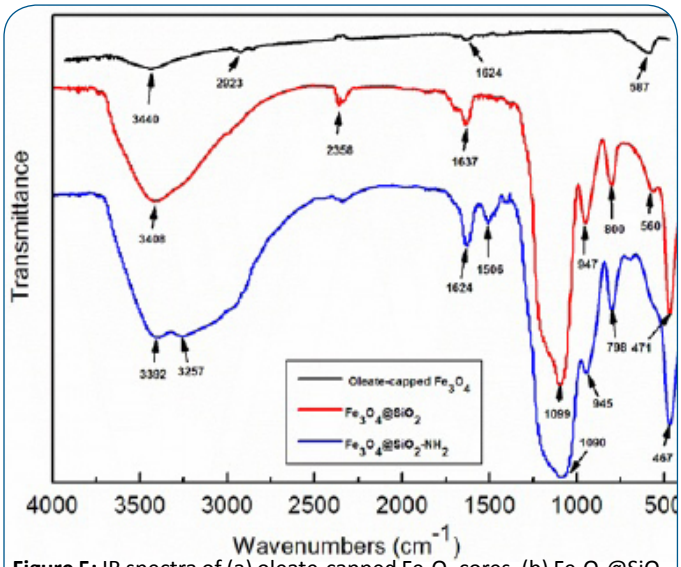

Figure 5: IR spectra of (a) oleate-capped Fe_3O_4 cores, (b) Fe_3O_4@SiO_2 core-shell nanoparticles, and (c) Fe_3O_4@SiO_2-NH_2 10% functionalized core-shell nanoparticles

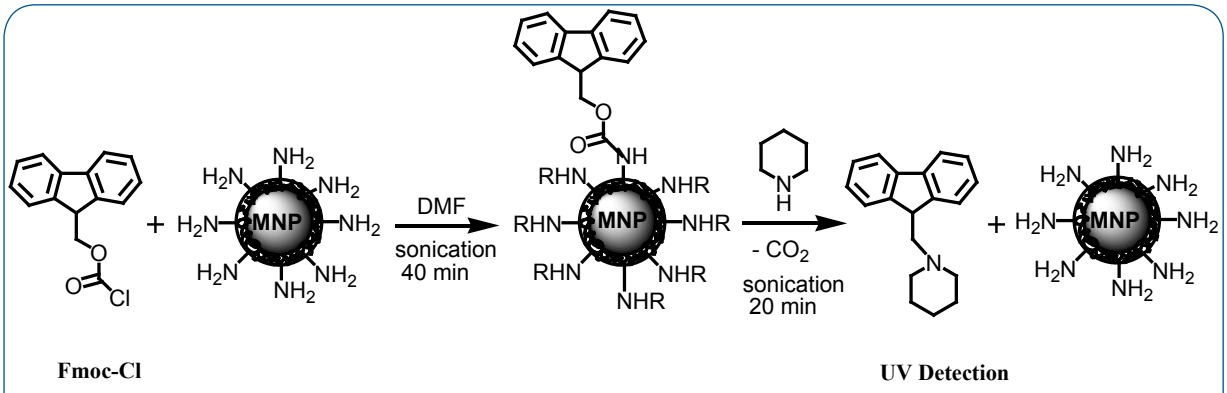

Scheme 2: Assay of active amine groups on Fe_3O_4@SiO_2-NH_2 nanoparticles

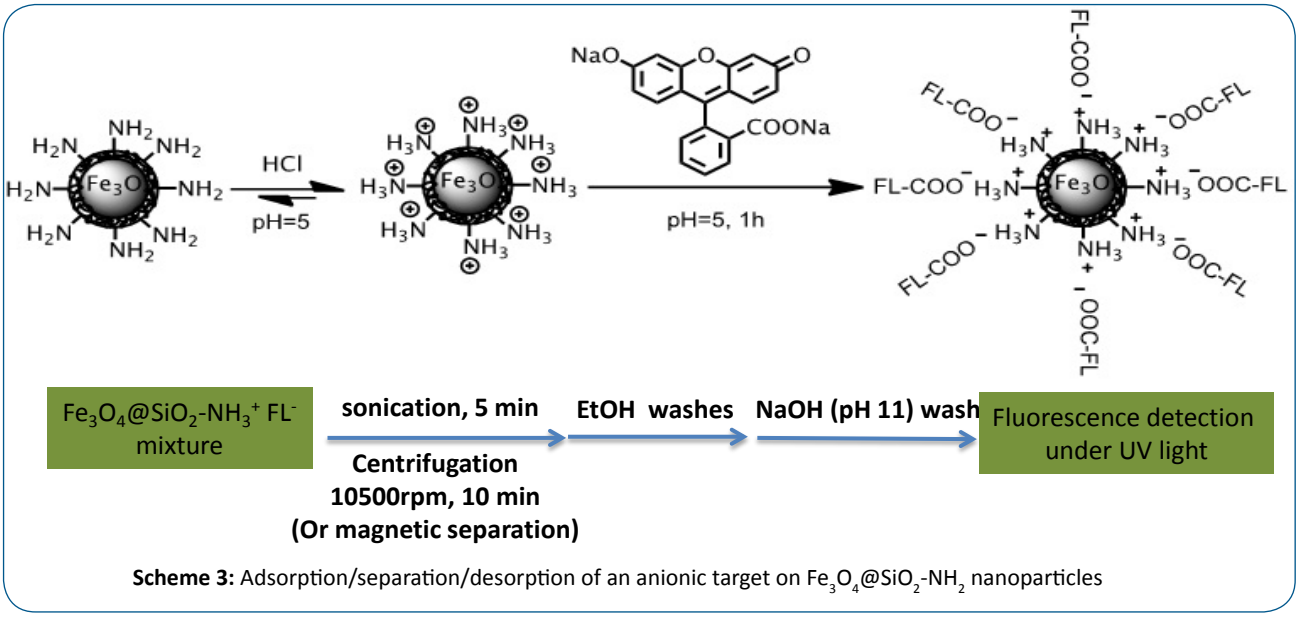

Scheme 3: Adsorption/separation/desorption of an anionic target on Fe_3O_4@SiO_2-NH_2 nanoparticles

phenolate form, causing the solution of released target to glow visibly under long-wave UV light. Fluorometric analysis of fluorescein concentration in the supernatant indicated an average of 2.73 x 10^3 adsorbed target molecules per nanoparticle, nearly six times lower than the number of active amine moieties, as determined by Fmoc quantification. This discrepancy is likely due to the difference in binding mechanism – the target is electrostatically bound, whereas the binding of Fmoc is covalent.

Conclusion

Core-shell structures of amine functionalized magnetic nanoparticles with tunable shell thickness have been successfully fabricated using a one-pot reverse microemulsion method. The nanoparticles prepared by this method are predominantly single-core and highly monodisperse. The silica shell can be readily functionalized with a wide variety of target-specific moieties, while the superparamagnetic core enables bound targets to be magnetically "fished-out" of a reaction mixture. Fluorescein was used as a model carboxylate molecule to demonstrate the potential separation ability of Fe_3O_4@SiO_2-NH_2 nanoparticles towards cationic targets. This system shows great promise for use in a closed-cycle magnetic purification (CCMP) microfluidic device.

References

1. Ho KM, Li P. Design and Synthesis of Novel Magnetic Core-Shell Polymeric Particles. Langmuir. 2008; 24:1801-1807. doi: http://dx.doi.org/10.1021/la702887m.
2. Chen W, Lu F, Chen C-CV, Mo K-C, Hung Y, Guo Z-X, et al. Manganese-enhanced MRI of rat brain based on slow cerebral delivery of manganese(II) with silica-encapsulated MnxFe(1-x)O nanoparticles. NMR Biomed. 2013; 26(9):1176-1185. doi: 10.1002/nbm.2932.
3. Boni A, Albertazzi L, Innocenti C, Gemmi M, Bifone A. Water dispersal and functionalization of hydrophobic iron oxide nanoparticles with lipid-modified poly(amidoamine) dendrimers. Langmuir. 2013; 29(35):10973-10979. doi: 10.1021/la400791a.
4. Budgin AM, Kabachii YA, Shifrina ZB, Valetsky PM, Kochev SS, Stein BD, et al. Functionalization of magnetic nanoparticles with amphiphilic block copolymers: self-assembled thermoresponsive submicrometer particles. Langmuir. 2012; 28(9):4142-4151. doi: http://dx.doi.org/10.1021/la205056k.
5. Xu S, Song X, Guo J,Wang C. Composite microspheres for separation of plasmid DNA decorated with MNPs through in situ growth or interfacial immobilization followed by silica coating. ACS Appl. Mater. Interfaces. 2012; 4(9):4764-4775. doi: http://dx.doi.org/10.1021/am301129n.
6. Majewski AP, Stahlschmidt U, Jérôme Vr, Freitag R, Müller AHE, Schmalz H. PDMAEMA-grafted core-shell-corona particles for nonviral gene delivery and magnetic cell separation. Biomacromolecules. 2013; 14(9):3081-3090. doi: 10.1021/bm400703d.
7. Ruhland TM, Lang JRV, Alt HG, Müller AHE. Magnetic Core-Shell Nanoparticles as Carriers for Olefin Dimerization Catalysts. Eur. J. Inorg. Chem. 2013; 2013(12):2146-2153. doi: http://dx.doi.org/10.1002/ejic.201201547.
8. Gage SH, Stein BD, Nikoshvili LZ, Matveeva VG, Sulman MG, Sulman EM, et al. Functionalization of monodisperse iron oxide NPs and their properties as magnetically recoverable catalysts. Langmuir. 2013; 29(1):466-473. doi: http://dx.doi.org/10.1021/la304410z.
9. Zimny K, Mascaro B, Brunet T, Poncelet O, Aristégui C, Leng J, et al. Design of a fluorinated magneto-responsive material with tuneable ultrasound scattering properties. J. Mater. Chem. B. 2014; 2(10):1285-1297. doi: http://dx.doi.org/10.1039/c3tb21585g.
10. Duong B, Khurshid H, Gangopadhyay P, Devkota J, Stojak K, Srikanth H, et al. Enhanced magnetism in highly ordered magnetite nanoparticle-filled nanohole arrays. Small. 2014; 10(14):2840-2848. doi: 10.1002/smll.201303809.
11. Chang Y, Yang C, Zheng X-Y, Wang D-Y, Yang Z-G. Fabrication of copper patterns on flexible substrate by patterning-adsorption-plating process. ACS Appl. Mater. Interfaces. 2014; 6(2):768-772. doi: 10.1021/am405539r.
12. Yang H, Zhuang Y, Hu H, Du X, Zhang C, Shi X, et al. Silica-Coated Manganese Oxide Nanoparticles as a Platform for Targeted Magnetic Resonance and Fluorescence Imaging of Cancer Cells. Adv. Funct. Mater. 2010; 20(11):1733-1741. doi: http://dx.doi.org/10.1002/adfm.200902445.
13. Huber DL. Synthesis, properties, and applications of iron nanoparticles. Small. 2005; 1(5):482-501.
14. Pfaff A, Schallon A, Ruhland TM, Majewski AP, Schmalz H, Freitag R, et al. Magnetic and fluorescent glycopolymer hybrid nanoparticles for intranuclear optical imaging. Biomacromolecules. 2011; 12(10):3805-3811. doi: http://dx.doi.org/10.1021/bm201051p.
15. Lu AH, Salabas EL, Schuth F. Magnetic nanoparticles: synthesis, protection, functionalization, and application. Angew. Chem. Int. Ed. 2007; 46(8):1222-1244.
16. Feng Z, Zhu S, Martins de Godoi DR, Samia ACS, Scherson D. Adsorption of Cd2+ on carboxyl-terminated superparamagnetic iron oxide nanoparticles. Anal. Chem. 2012; 84(8):3764-3770. doi: 10.1021/ac300392k.
17. Turcheniuk K, Tarasevych AV, Kukhar VP, Boukherroub R, Szunerits S. Recent advances in surface chemistry strategies for the fabrication of functional iron oxide based magnetic nanoparticles. Nanoscale. 2013; 5(22):10729-10752. doi: 10.1039/c3nr04131j.
18. Bee A, Massart R, Neveu S. Synthesis of very fine maghemite particles. J. Magn. Magn. Mater. 1995; 149(1-2):6-9. doi:10.1016/0304-8853(95)00317-7.
19. Sun S, Zeng H, Robinson DB, Raoux S, Rice PM, Wang SX, et al. Monodisperse MFe2O4 (M) Fe, Co, Mn) Nanoparticles. J. Am. Chem. Soc. 2004; 126(1):273-279.
20. Park J, An K, Hwang Y, Park JG, Noh HJ, Kim JY, et al. Ultra-large-scale syntheses of monodisperse nanocrystals. Nat. Mater. 2004; 3(12):891-895. doi: http://dx.doi.org/10.1038/nmat1251.
21. Solinas S, Piccaluga G, Morales MP, Serna CJ. Sol-Gel Formation of γ-Fe2O3/SiO2 Nanocomposites. Acta mater. 2001; 49(14):2805-2811. doi:10.1016/S1359-6454(01)00160-4.
22. Deng H, Li X, Peng Q, Wang X, Chen J, Li Y. Monodisperse magnetic single-crystal ferrite microspheres. Angew. Chem. Int. Ed. 2005; 44(18):2782-2785.
23. Ling D, Hyeon T. Chemical design of biocompatible iron oxide nanoparticles for medical applications. Small. 2013; 9(9-10):1450-1466. doi: 10.1002/smll.201202111.
24. Yu K, Zhang X, Tong H, Yan X, Liu S. Synthesis of fibrous monodisperse core–shell Fe3O4/SiO2/KCC-1. Mater. Lett. 2013; 106:151-154. doi:10.1016/j.matlet.2013.04.112.
25. Deng M, Tu N, Bai F, Wang L. Surface Functionalization of Hydrophobic Nanocrystals with One Particle per Micelle for Bioapplications. Chem. Mater. 2012; 24(13):2592-2597. doi: http://dx.doi.org/10.1021/cm301285g.

26. Liu Y, Chen T, Wu C, Qiu L, Hu R, Li J, et al. Facile surface functionalization of hydrophobic magnetic nanoparticles. J. Am. Chem. Soc. 2014; 136(36):12552-12555. doi: http://dx.doi.org/10.1021/ja5060324.

27. Wu W, He Q, Jiang C. Magnetic iron oxide nanoparticles: synthesis and surface functionalization strategies. Nanoscale. Res. Lett. 2008; 3(11):397-415. doi: 10.1007/s11671-008-9174-9.

28. Laurent S, Forge D, Port M, Roch A, Robic C, Vander Elst L, et al. Magnetic Iron Oxide Nanoparticles: Synthesis, Stabilization, Vectorization, Physicochemical Characterizations, and Biological Applications. Chem. Rev. 2008; 108(6):2064-2110. doi: 10.1021/cr068445e.

29. Barroso T, Casimiro T, Ferraria AM, Mattioli F, Aguiar-Ricardo A, Roque ACA. Hybrid Monoliths for Magnetically-Driven Protein Separations. Adv. Funct. Mater. 2014; 24(28):4528-4541. doi: http://dx.doi.org/10.1002/adfm.201400022.

30. Feng G, Jiang L, Wen P, Cui Y, Li H, Hu D. A new ion-exchange adsorbent with paramagnetic properties for the separation of genomic DNA. Analyst. 2011; 136(22):4822-4829. doi: 10.1039/c1an15149e.

31. Xu H, Aguilar ZP, Yang L, Kuang M, Duan H, Xiong Y, et al. Antibody conjugated magnetic iron oxide nanoparticles for cancer cell separation in fresh whole blood. Biomaterials. 2011; 32(36):9758-9765. doi: 10.1016/j.biomaterials.2011.08.076.

32. Fu X, Chen X, Wang J, Liu J. Fabrication of carboxylic functionalized superparamagnetic mesoporous silica microspheres and their application for removal basic dye pollutants from water. Microporous Mesoporous Mater. 2011; 139(1-3):8-15. doi: http://dx.doi.org/10.1016/j.micromeso.2010.10.004.

33. Odio OF, Lartundo-Rojas L, Santiago-Jacinto P, Martínez R, Reguera E. Sorption of Gold by Naked and Thiol-Capped Magnetite Nanoparticles: An XPS Approach. J. Phys. Chem. C. 2014; 118(5):2776-2791. doi: http://dx.doi.org/10.1021/jp409653t.

34. Jiang F, Fu Y, Zhu Y, Tang Z, Sheng P. Fabrication of iron oxide/silica core–shell nanoparticles and their magnetic characteristics. J. Alloys Compd. 2012; 543:43-48. doi:10.1016/j.jallcom.2012.07.079.

35. Vogt C, Toprak MS, Muhammed M, Laurent S, Bridot J-L, Müller RN. High quality and tuneable silica shell–magnetic core nanoparticles. J. Nanopart. Res. 2009; 12(4):1137-1147. doi: http://dx.doi.org/10.1007/s11051-009-9661-7.

36. Koole R, van Schooneveld MM, Hilhorst J, de Mello Donegá C, Hart DCt, van Blaaderen A, et al. On the Incorporation Mechanism of Hydrophobic Quantum Dots in Silica Spheres by a Reverse Microemulsion Method. Chem. Mater. 2008; 20:2503–2512. doi: http://dx.doi.org/10.1021/cm703348y.

37. Ding HL, Zhang YX, Wang S, Xu JM, Xu SC, Li GH. Fe3O4@SiO2Core/Shell Nanoparticles: The Silica Coating Regulations with a Single Core for Different Core Sizes and Shell Thicknesses. Chem. Mater. 2012; 24(23):4572-4580. doi: http://dx.doi.org/10.1021/cm302828d.

38. Wang J, Shah ZH, Zhang S, Lu R. Silica-based nanocomposites via reverse microemulsions: classifications, preparations, and applications. Nanoscale. 2014; 6(9):4418-4437. doi: 10.1039/c3nr06025j.

39. Yathindranath V, Sun Z, Worden M, Donald LJ, Thliveris JA, Miller DW, et al. One-pot synthesis of iron oxide nanoparticles with functional silane shells: a versatile general precursor for conjugations and biomedical applications. Langmuir. 2013; 29(34):10850-10858. doi: 10.1021/la402007d.

40. Kaulen C, Homberger M, Bourone S, Babajani N, Karthauser S, Besmehn A, et al. Differential adsorption of gold nanoparticles to gold/palladium and platinum surfaces. Langmuir. 2014; 30(2):574-583. doi: http://dx.doi.org/10.1021/la404110y.

41. Guo S, Dong S, Wang E. A general route to construct diverse multifunctional Fe3O4/metal hybrid nanostructures. Chem. Eur. J. 2009; 15(10):2416-2424. doi: 10.1002/chem.200801942.

42. Zhu Z, Wei X, Xu F, Wang Y. Synthesis and characterization of amino-functionalized single magnetic core–silica shell composites. Solid State Sci. 2012; 14(10):1550-1556. doi:10.1016/j.solidstatesciences.2012.08.017.

43. Yoon TJ, Yu KN, Kim E, Kim JS, Kim BG, Yun SH, et al. Specific targeting, cell sorting, and bioimaging with smart magnetic silica core-shell nanomaterials. Small. 2006; 2(2):209-215.